TOC Reduction in Drinking Water using Anionic Surfactant Modified Bentonite

Farida M. S. E. El-Dars[1]*, M. Y. M. Hussein[2], A. H. T Kandil[1]

[1] Chemistry Department, Faculty of Science, Helwan University, Helwan, 11795 Cairo, Egypt.
[2] The Holding Company for Water and Wastewater (HCWW) - Cairo - Egypt.
* *Corresponding authors. E-mail: fkeldars@hotmail.com*

Abstract- The removal of Total organic carbon (TOC) from liquid solution using Na-bentonite (Na-B) and anionic sodium dodecyl sulfate surfactant modified bentonite (SDS-B) was investigated. B atch studies were carried out to investigate the effect of experimental parameters including the initial solution pH, contact time, temperature, and adsorbent dose upon the adsorption process. The experimental data was well represented by a second order kinetics model for both types of bentonite. However, the process was found to involve some degree of intra-particle diffusion for SDS-B adsorption and intraparticle plus pore diffusion for Na-B. Based upon the kinetic modeling, the calculated energies of activation for the process was - 49.06 kJ/mol and -22.41 kJ/mol for Na-B and SDS-B, respectively. The data also indicated that the process of adsorption onto both materials was better fitted to the Freundlich model. The thermodynamic parameters (ΔH°, ΔS° and ΔG°) were calculated and they indicated that the process was exothermic and spontaneous and in the forward direction for SDS-bentonite and was spontaneous in the reverse direction for Na-bentonite. .

Index Terms: TOC reduction, anionic surfactant modified bentonite, adsorption, thermodynamics.

1 INTRODUCTION

NOM is a complex mixture of organic compounds that exists in all natural waters as a result of the interactions between the hydrological cycle with the biosphere and geo-sphere [1],[2]. The amount, character and properties of NOM differ considerably in waters of different origins and depend on the biogeochemical cycles of the surrounding environments [3]. In effect, while NOM is responsible for the color; taste and odor problems associated with water sources, it may also be a carrier of metals and hydrophobic organic chemicals [2]. As well, it may have a corrosive effect and act as a substrate for bacterial growth in the water distribution system if not controlled.

Generally and in a water treatment plant, the presence of NOM affects the performances of the unit processes, the application of water treatment chemicals as well as the biological stability of water before and after treatment [2],[4]. However, it is that change in quantity and quality of NOM in natural waters that has a significant influence upon the selection, design and operation of water treatment processes [2]. Effectively, while the majority of coagulants added and disinfectants used target the removal of NOM from these waters, the seasonal variability and increase in NOM imposes serious challenges to water treatment facilities in terms of operational optimization and proper process control [5]. As well, NOM has a tendency to interfere with the removal of other contaminants. Health-wise, both the hydrophobic and hydrophilic components of NOM were reported to be the major contributors towards the formation of disinfection by-products, that have been recently associated with serious health effects [2], [4], [5].

Total organic carbon (TOC) - the sum of the particulate and dissolved organic carbon (DOC) - is the most convenient parameter used to attest the efficiency of a treatment processes and its effects on NOM removal (Kristiana et al., 2011). This is because it was reported that the hydrophobic high molecular weight content (the largest fraction) of NOM which is the most important pre-cursors for DBP formation constituted almost 50% of raw water TOC [5], [6]. In other words, a significant reduction in the total organic carbon (TOC) of the treated waters is considered a viable indicator for NOM removal.

However, with the increasingly stringent DBP regulations being adopted, there is a need for advanced precursor removal technologies that lead to maximum NOM removal. Generally, the most common and economically feasible processes used for the removal of NOM are coagulation and flocculation followed by sedimentation/flotation and sand filtration [7]. Most of the NOM in natural waters were reported to be removed by coagulation with inorganic aluminum and iron salts [6] or enhanced coagulation under different TOC and alkalinity levels (Xiao et al., 2010). However, the effectiveness of coagulation to remove NOM and particles depends on several factors. These include the coagulant type and dosage, mixing conditions, pH, temperature, particle and NOM properties (such as size, functionality, charge and hydrophobicity), as well as the presence of divalent cations and concentrations of destabilizing anions (bicarbonate, chloride, and sulfate). Nonetheless, one of the disadvantages of using these chemicals is the potential for application of high coagulant dosages which may not be effective for the removal and may increase water turbidity. Therefore, new developed inorganic polymer flocculants (IPFs) based on inorganic salts were being introduced within the past few years. As well, other alternatives for NOM removal were re-

- *M. Y. M. Hussien is currently pursuing masters degree program in analytical and inorganic chemistry at Helwan University, Helwan, Cairo, Egypt. E-mail: elaraby2941987@yahoo.com*

International Journal of Scientific & Engineering Research Volume 6, Issue 3, March-2015
ISSN 2229-5518

cently being explored that included ion exchange and membrane filtration (microfiltration, nanofiltration, reverse osmosis) [4], [9].

From an environmental point of view, adsorption offers significant advantages over traditional treatment methods as it may provide for better and safer removal of organic contaminants from wastewater [10], [11]. Of all the sorbents tested, activated carbon (granular activated carbon and powdered activated carbon (PAC)), is the best and most widely used due to its porous nature and large internal surface area [9], [11]. However, of the disadvantages of the application of activated carbons is its high price and that there is not possibility of reuse or regeneration [10], [12].

On the other hand, there has been a recent and increasing interest for the utilization of natural clay materials in the removal of toxic metals and some organic pollutants from aqueous solutions [13]. One type of these clay minerals is bentonite, which exists as discrete deposits in most continents of the world. Bentonite is a rich clay mineral that consists of layers made up of an octahedral alumina sheet sandwiched between two tetrahedral silica sheets [13]. The wide use of bentonite as a low cost sorbent may be attributed to its high surface area, high chemical and mechanical stability and to a variety of surface and structural properties [13], [14]. However, natural bentonite weakly adsorbs anionic pollutants because of the repulsion between the anion and the negative charge on the edge of the bentonite sheet [15]. As well, and because of its hydrophilicity, the contaminant uptake by this type of clay is rather low [7]. Thus, modification of bentonite surface properties has been considered in order to improve upon its cation and anion adsorption capacity.

In effect, surfactants modified bentonites were reported to be efficient in treatment of various pollutants [14]. A number of studies have shown that these organo-bentonite were a promising emerging class of sorbents that was effective in the removal of organic contaminants from some wastewaters [11], [16], [17]. This change in adsorbing properties of bentonite was attributed to the intercalation of surfactant between the clay layers as the addition of surfactants to the suspension of bentonite was found to enhance its rheological properties [16], [17], [18]. Surfactant adsorption onto clay also causes structural changes on adsorbents clay minerals which do affect the pore structure, surface properties, and adsorptive behavior of surfactant modified adsorbents [11], [16], [17], [19]. Thus, by partition onto the organic phase created by the intercalated surfactant, organic contaminants may be removed effectively by modified bentonite. However, this ability of surfactant to adsorb at the solid/liquid interface was controlled by chemical nature of the components of the system: the solid, the surfactant, and the medium [14].

With no literature available concerning the use of anionic surfactant modified bentonite for TOC reduction in drinking waters, this work aims at studying the adsorptive capabilities of sodium dodecyl sulfate modified bentonite (SDS-B) upon TOC removal form aqueous solutions. The change in adsorbent structure of this modified bentonite was characterized relative to Na-B and the capacities for adsorption of both materials for the removal of TOC from solution were evaluated. The effect of different operating parameters on these adsorption processes, such as dose of adsorbent, the initial pH value, temperature and the contact/shacking time were studied in batch process and the data was used to elucidate the kinetics, thermodynamics and adsorption isotherm parameters of the studied process.

2 MATERALS AND METHODS

2.1 Preparation of Na-Bentonite (Na-B):

Na-bentonite was prepared according to the method described by Al-Asheh et al. [13]. Powder pure bentonite (Ferro Chemicals, Egypt) was soaked in 1M NaCl solution (Sigma Aldrich, USA) and then washed several times with distilled water until it was chloride free. The process was checked by the addition of $AgNO_3$ solution (Sigma Aldrich, USA) to the resulting water to make sure that no precipitate was formed. This chemical treatment was intended to offset the charge unbalance on the clay before use. The solid particles were separated from solution by filtration, dried at 70 °C, and stored until further use. This bentonite was designated as Na-bentonite (Na-B) and was used for further adsorption tests.

2.2 Preparation of Anionic Surfactant Modified Bentonite (SDS-B):

The prepared Na-bentonite was treated with an anionic surfactant for the purpose of surface enhancement. Sodium dodecyl sulfate [SDS; $CH_3(CH_2)_{10}CH_2OSO_2ONa$] (Sigma Aldrich, USA) was used to prepare the SDS modified bentonite according to the method described by Al-Asheh et al. [13]. 200 mL of 4% of SDS solution were prepared by dissolving of an appropriate weight in distilled water. 20 g of the prepared Na-bentonite was added to the solution and the mixture was mechanically stirred for 48 h. The anionic surfactant modified bentonite (SDS-B) was separated from the solution by filtration, washed twice with distilled water, dried at 70 °C, and stored for further use in the adsorption tests. Table 1 shows the chemical characteristics of both the Na-Bentonite and SDS-bentonite prepared as well as the XRD and FTIR analysis of both sorbent materials are shown in Figs 1 and 2, respectively.

2.3 TOC Sample Preparation:

Total Organic Carbon (TOC) measurements are typically used to quantify NOM concentrations water samples [20]. Anhydrous potassium biphtalate ($C_8H_5KO_4$) (Panreac Quimica, Spain) was used to simulate the TOC concentration of the tested waters [21]. A stock standard solution of potassium biphtalate was prepared in carbon free water and was used to obtain TOC concentrations of 10-12 mg/L, which is comparable to the monthly range TOC values obtained for raw Nile waters during a full year survey from August 2012- July 2013. TOC solutions prepared within this concentration range were used for the optimization and removal studies.

International Journal of Scientific & Engineering Research Volume 6, Issue 3, March-2015
ISSN 2229-5518

TABLE 1
CHEMICAL ANALYSIS OF NA-B AND SDS-B (%WT/WT)

Characteristic	Na-Bentonite (% w/w)	SDS-Bentonite (%w/w)
SiO_2	55.50	37.8
Al_2O_3	13.90	9.00
Fe_2O_3	4.20	2.56
CaO	3.20	2.70
MgO	5.03	3.22
SO_3	0.10	8.30
Cl	0.073	0.80
Na_2O	2.10	0.50
K_2O	1.22	0.95
L.O.I	13.90	32.86

2.4 Kinetics and equilibrium experiments:

Batch adsorption experiments were carried out in a thermostated water bath/shaker at a constant temperature. The effect of contact time, solution pH, adsorbent dose and temperature were studied for each adsorbent. 50 mL of TOC solution of known concentration (10-12 mg/L) were shaken with different weights of adsorbent material (0.125–1.0 g) at different temperatures (25 - 60ºC) for various mixing time (1-240 min) and throughout the pH range of (5-12). Separation of the solid phase from liquid was achieved by centrifuging for 15 min (3500 rpm) followed by filtration. The filtrates were analyzed for the residual TOC concentration using TOC analyzer (GE, Sievers, model no.5310C, USA) according to APHA [21]. The % of TOC uptake was calculated as follows:

$$\%\ \text{TOC uptake} = [C_0 - C_t / C_0] \times 100 \quad (1)$$

where C_0 and C_t are the initial and final concentration of TOC in solution (mg/L), respectively. The amount of TOC accumulated per unit mass of adsorbent was evaluated using the following equation [22]:

$$q_t = (C_0 - C_t)\, V / m \quad (2)$$

where m is the weight of sorbent used (g) and V is the volume of TOC solution (L). At equilibrium contact time t_e, Ct becomes C_e and the amount of TOC sorbed (q_t) is equivalent to amount at equilibrium (q_e).

To a series of 150 mL capacity tubes containing the desired amount of TOC solution of known concentrations, a predetermined amount of each adsorbent was added and the mixture was agitated in a thermostated water bath-shaker. At set time intervals, the solutions were filtered and the TOC concentration was determined. Thermodynamic parameters (ΔH^o, ΔG^o and ΔS^o) were calculated from the adsorption results. The optimal weight of each adsorbent material/L was added to a solution of known TOC concentration at pH 5 and was shaken for 50 minutes (SDS-bentonite) and 100 minutes (Na-bentonite) at different temperatures.

3 RESULTS AND DISCUSSION

3.1 Characterization of Na-Bentonite and SDS-Bentonite

FTIR spectroscopy is an important technique used in identifying characteristic surface functional groups on the adsorbent, which in some cases may be responsible for the binding of the adsorbate molecules [12]. The surface functional groups of Na-B and SDS-B were detected by FTIR and the spectra was recorded from 4000 to 400 cm^{-1}. The FTIR obtained for Na-bentonite and SDS- bentonite is shown in Figs 1(a) and (b). For Na-bentonite, the peak at 3627 cm^{-1} was reported to indicate Al–Al–OH stretching vibration typical of smectites with high amount of Al in the octahedral layer [18]. In addition, this peak was reported to be associated with the stretching vibration of the structural group of –OH of bentonite [23]. The peaks at 3460 and 1642 cm^{-1} indicate the O–H stretching and bending vibrations for the adsorbed water, respectively [23]. Sharp peak at 1028 cm^{-1} was attributed to the Si–O stretching frequency as well as the bands at 516 and 455 cm^{-1} correspond to Al–O–Si and Si–O–Si bending vibrations as well as the tetrahedral bending mode for Si–O–Al.

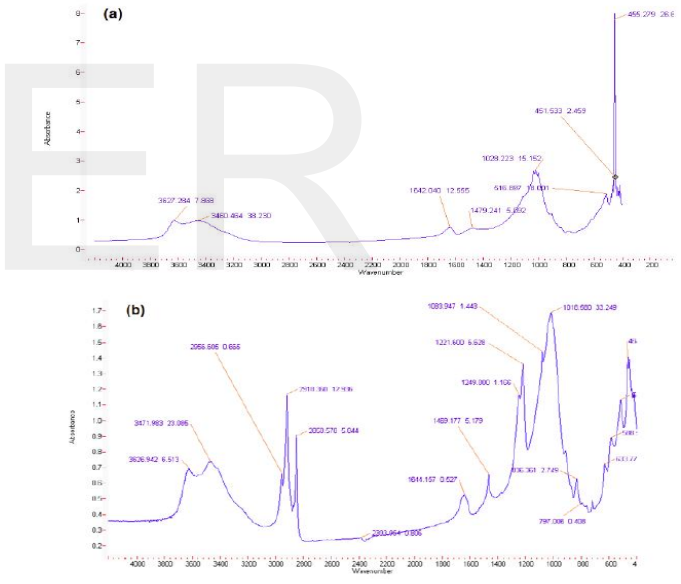

Fig. 1. FTIR spectra of (a) Na-Bentonite and (b) SDS-Bentonite

It was reported that surfactant adsorption onto clay minerals may cause structural changes in its interlayer arrangement that affects the pore structure, surface properties, and adsorptive behavior of surfactant modified adsorbents [19]. FTIR of the prepared SDS-Bentonite shown in Fig. 1(b) indicates that the O–H stretching or bending bands recorded for Na-bentonite at 3627, 3460 and 1642 cm^{-1} were shifted to 3626, 3471 and 1644 cm^{-1} for SDS-bentonite, which is in agreement with the results obtained by Tunç et al. [18]. These bands were indicative of the O-H stretching or bending bands of the Na-bentonite-SDS system. In addition, the new bands that appeared at 2918, 2850 and 1469 cm^{-1} were reported to be due to the interaction of the clay with the anionic surfactant as well

International Journal of Scientific & Engineering Research Volume 6, Issue 3, March-2015
ISSN 2229-5518

the stretching vibrations of C-H of pure anionic surfactant. In addition, the sharp peak obtained at 1028 cm^{-1} representing the Si–O stretching in Na-bentonite was shifted to 1018 cm^{-1} after surfactant modification of the clay's surface. The peaks at 2851 and 2917 cm^{-1} may be assigned to the aliphatic C–H stretching vibration [23]. A band at 633 cm^{-1} was assigned to the out-of-plane vibrations of coupled Al–O and Si–O. A number of bands that appeared within the SDS-B spectrum include the asymmetric (CH_3) stretching vibrational band at 2956 cm^{-1}, the asymmetric and symmetric CH_2 stretching vibrational frequencies at 2918 and 2850 cm^{-1}, and the (CH_2) band at 1469 cm^{-1} which is a characteristic of partially ordered chains [24] or of the deformation of the bands of the methyl and methylene groups [25]. It was reported that when the $\nu_{sym}(CH_2)$ band had values lower than 2852 cm^{-1}, it was a good indication of the more ordered crystalline structure, while values higher than that were representative of micelles and liquid crystals. As well, the spectrum showed no shoulder at 2860 cm^{-1} which indicates the absence of non crystallized SDS or hydrated crystalline SDS within the prepared SDS-bentonite [24], [25]. In addition, the overlapping of the bands at 1221 and 1249 cm^{-1} may be due to S–O stretching and the separation between these two peaks may be indicative of the change in the conformational structure, which is in agreement with the results reported by Viana et al. [24]. Conclusively, the above data indicate that the interaction of SDS with Na-bentonite was achieved through the formation of hydrogen bonding between the clay particles and the surfactant molecules [18].

The XRD obtained for both adsorbent materials is shown in Figs 2 (A) and (B). For Na-bentonite, the basal spacing obtained was 13.42 Å compared which varied from the reported value for natural bentonite (12.12 Å) indicating the saturation of the clay with Na^+. As well, there was an increase in the basal spacing for SDS-bentonite from 13.42 to 20.78 Å relative to Na- bentonite. This increase may be attributed to the intercalation of the SDS into the bentonite which caused the bentonite to swell [26], [27], [28]. This intercalation of SDS into bentonite was revealed in Fig. 2 (b) as new peaks indicative of the presence of sodium lauryl sulfate bound to bentonite appeared in the difractogram. As well, the diffusion of surfactant molecules through the interlayer sheets of bentonite may have weaken the attraction forces between binding silicate sheets in the crystalline structure as the hydrophobic tails of SDS molecules attached itself to the positive edges of clay particles to disallow its interaction with one another [26]. Subsequently, this increases the surface area of bentonite as well as the spacing between the bentonite/clay sheets [13], [14], [26]. Accordingly, the obtained increase in basal spacing of bentonite after SDS modification may be indicative of the fact that more sites were made accessible for adsorption.

The results for particle size distribution for both Na-bentonite and SDS-bentonite are shown in Figs 3(a) and 3(b). The figures indicate that Na-bentonite had a particle size of 735.3 nm while that for SDS-bentonite; the particle size distribution was 142.6 nm (90%), which reflect a higher surface area for SDS-bentonite over Na-bentonite. This is accordance with the findings of Omar et al. [29] and Akl et al. [30] who indicated that organic /surfactant modified bentonite varied from the unmodified in particle size as well as in the relative surface area. As well, this reduction in particle size may be attributed to the fact that the addition of anionic surfactants to clay minerals caused a decrease in the electrostatic attraction between clay particles which lead to a steric push between the SDS covered clay particles [26], [31].

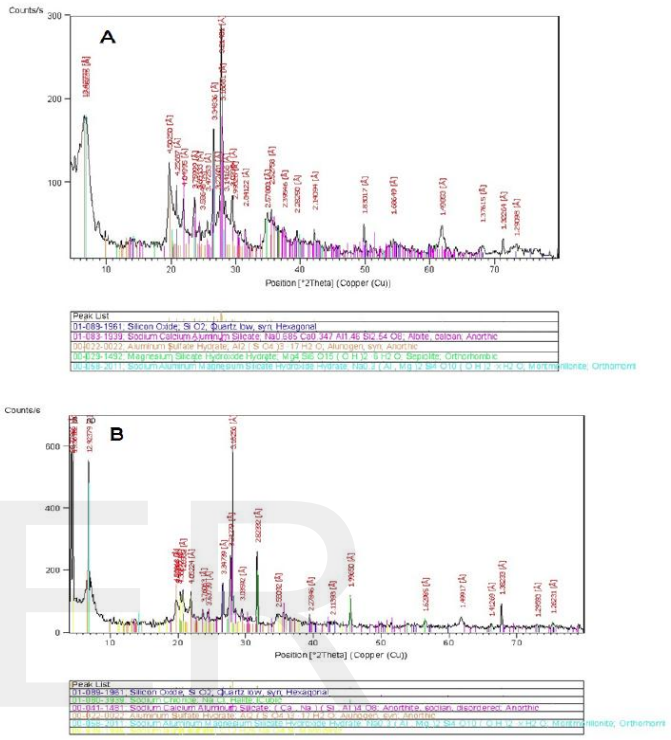

Fig. 2. XRD for (A) Na-Bentonite and (B) SDS-Bentonite

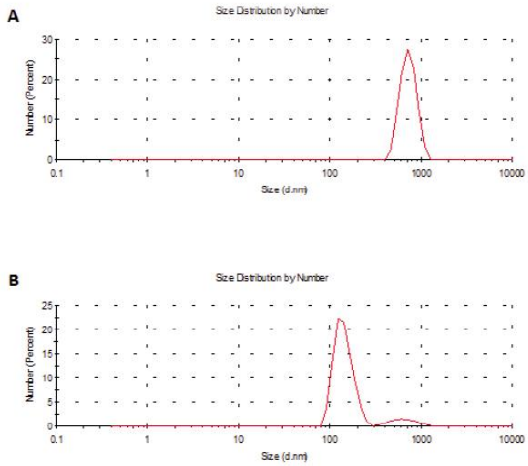

Fig. 3. Particle Size distribution for (A) Na-Bentonite and (B) SDS-Bentonite

International Journal of Scientific & Engineering Research Volume 6, Issue 3, March-2015
ISSN 2229-5518

3.2 Effect of varying adsorbent dose:

The effect of varying the Na-bentonite and SDS-bentonite dose upon the TOC reduction in solution is shown in Fig 4. The results indicate that a maximum TOC reduction of 7.96% and 97.87% was achieved using Na-bentonite and SDS-bentonite, respectively. However, it was observed that 5 g/L SDS-bentonite achieved an initial TOC reduction of 93.93%, which provided for a maximum adsorbent capacity of 2.37 mg/g. Alternatively, at a 5 g/L Na-bentonite dose, the maximum adsorbent capacity obtained was 1.39 x 10^{-1} mg/g as well as it required a 20 g/L dose to achieve an overall 8.0% TOC reduction. Similar trends of adsorption efficiency/ capacity for modified and unmodified bentonite in the removal of organic and inorganic pollutant were reported by Al-Asheh et al. [13], Anirudhan and Ramachandran [16] and Omar et al. [29]. It was indicated that the relatively higher removal efficiencies achieved by the modified bentonite was due to its ability to surround the pollutant molecules thus allowing them to be better attached to the clay surface [13], [14]. As well, the increase in SDS-B TOC removal % from solution may be attributed to the hydrophobic nature and high surface area of the modified bentonite relative to the Na-B [16]. In addition, it was speculated that the increase in interlayer spacing values -indicated here by XRD data- for the modified bentonite increased the sorbent surface accessibility for pollutant removal. On the other hand, in their study of the removal of humic acid (measured as BOD) from wastewaters, Anirudhan and Ramachandran [16] reported that maximum removals of 78.9% and 99.6% required the use of 17 g/L of Na-bentonite and 30g/L of (HDTMA) cationic surfactant modified bentonite, respectively. Nonetheless, in the current study, the optimal dose was 5 g/L of SDS-B and 20 g/L Na-B, which was used in further experimental work. This low dose of SDS-B, apart from being effective, may not pose any further health risks or cause foaming to hinder TOC removal from solution or add to its organic pollutant load.

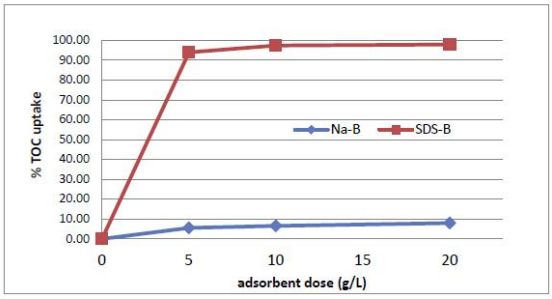

Fig. 4. The effect of varying of Na-B and SDS-B dose upon TOC% reduction in solution (pH 5, $t_{Na\text{-}B}$ =100 min, $t_{SDS\text{-}B}$ =50 min,T= 25 °C, vol= 50 mL and TOC_0= 12.612 mg/l)

3.3 The effect of contact /shaking time:

The effect of varying the contact time (0- 240 min) upon the TOC % uptake using Na-B and SDS-B was studied as a batch process and the results are shown in Fig. 5. It was observed that Na-bentonite showed a slight increase in TOC removal from 2.35% to 8.45% over the entire time range. However, SDS-bentonite achieved an initial maximum 96.35% TOC reduction after the initial 30 minutes; a value that remained constant thereafter indicating that equilibrium was reached. A similar equilibrium time of 40 min was obtained by Özcan et al. [10] during their study of the removal of synthetic reactive dyes using cationic modified bentonite. Nonetheless, in the current study, the data revealed that the equilibrium capacity for Na-B was 1.48 x 10^{-2} mg/g meanwhile that for SDS-B reached 2.43 mg/g. The lower value for q_e for Na-B may be indicative of the weak adsorption of TOC onto the material [27]. As well, it may indicate that the unmodified clay had a high hydrophobicity which impacted its uptake capacity towards organic contaminants [7]. The results also indicated that the adsorption of TOC onto SDS-bentonite was rapid at the first stage, which may suggest that the adsorption occurred mainly at the surface of the solid sorbent until surface saturation was reached [12], [32]. Al-Asheh et al. [13] and Ghazy et al. [32] postulated that this fast adsorption stage was followed by a slower stage which involved intraparticle diffusion to reach an equilibrium stage. As well, the current results indicate that the time required to reach equilibrium for TOC adsorption onto SDS-B was relatively shorter than that for Na-B. This relatively long contact time required by Na-B may be associated with mass transport and a slow diffusion mechanism of TOC molecules inside the microporous structure of Na-B [16].

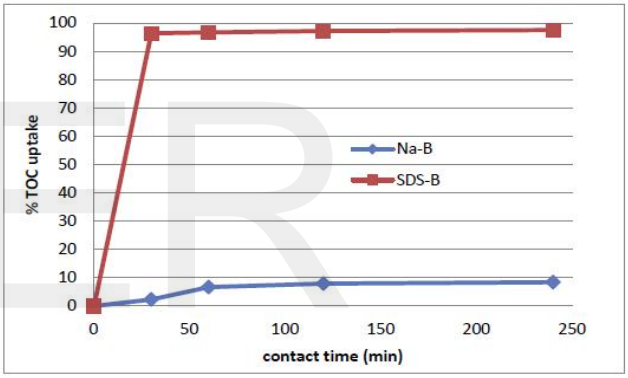

Fig. 5. The effect of varying the shaking time (min) upon % TOC reduction at pH 5, adsorbent dose: 20 g/L Na-B and 5 g/L SDS-B, T= 25 °C, vol= 50 mL and TOC_0= 12.6129 mg/l)

3.4 The effect of pH:

The pH of the aqueous solutions plays an important role in the whole adsorption process and particularly on the adsorption capacity [33]. The effect of pH upon TOC reduction in solution using Na-B and SDS-B was studied by varying the initial pH from 5.0–12.0. The results depicted in Fig. 6 indicate that the maximum TOC reduction of 86.99% and 11.18% was obtained at pH= 5 for Na-bentonite and SDS-bentonite, respectively. The decrease in TOC removal with the increase in pH may be due to the appearance of the negatively charged OH^- which may increase the ionic repulsion between the TOC molecules as well as compete with the anionic surfactant on clay [10], [30]. This is accordance with the findings of Syafalni et al. [34] who reported that the modification of bentonite with anionic surfactant increased the negative charge on the clay which affected the adsorption of organic pollutants rather than H^+ ions in solution. More specifically, it was reported that un-dissociated molecules that dominated at low pH were hydrophobic and more absorbable than the ionized form [16].

International Journal of Scientific & Engineering Research Volume 6, Issue 3, March-2015
ISSN 2229-5518

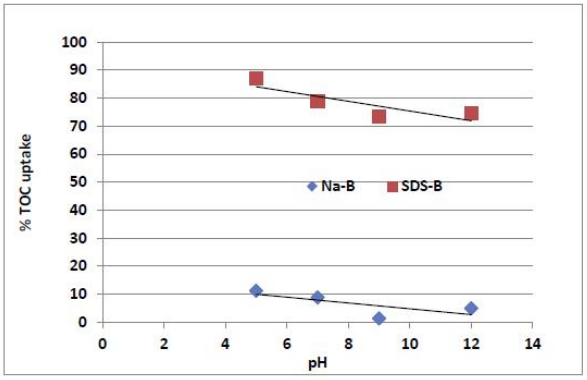

Fig. 6. The effect of varying the pH upon % TOC reduction using the adsorbent doses of: 20 g/L Na-B and 5 g/L SDS-B, t_{Na-B} =60 min, t_{SDS-B} =30 min,T= 25 °C, vol= 50 mL and TOC_0= 12.20 mg/L)

3.5 The effect of temperature:

Temperature is one of the parameters that significantly influence the rate of reaction [22]. The relationship between the %TOC uptake by SDS-bentonite and Na-bentonite at different temperatures (25-60°C) was investigated and the results are illustrated in Fig. 7. It is clear from Fig 7 that SDS-bentonite achieved higher adsorption rates (over 92%) relative to Na-bentonite which achieved a maximum of 6.74% at 25°C. Effectively, from the data it was apparent that the % TOC uptake for both SDS-B and Na-B decreased with the increase of temperature. As well, the adsorption capacity for SDS-bentonite and Na-bentonite decreased from 2.024 to 1.953 mg/g and 0.035 to 0.027 mg/g going from 25 °C to 60 °C, accordingly. Similar thermal behavior was reported by Atia et al. [14] and it was attributed to the fact that anionic surfactants were physically adsorbed onto the surface of bentonite through ion exchange and that the high energy resulting from the increase in temperature may enhance the removal of surfactant molecules from the surface. In addition, the decrease in adsorption with the increase in temperature was attributed to the weakening of the adsorptive forces between the active sites of the adsorbent and adsorbate species and also between the adjacent molecules of the adsorbed phase [16].

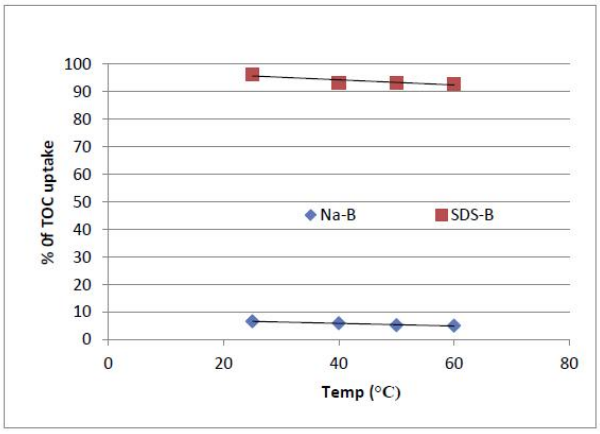

Fig. 7. The effect of varying the temperature (°C) upon % TOC reduction at pH 5, adsorbent dose: 20 g/L Na-B and 5 g/L SDS-B, t_{Na-B} =60 min, t_{SDS-B} =30 min, vol= 50 mL and TOC_0= 10.5 mg/L)

3.6 Adsoprtion Isotherm:

An adsorption isotherm shows the equilibrium relationship between the concentration in the fluid and onto the adsorbent at constant temperature [35]. As well, sorption isotherms represent the relationship between the amount adsorbed by a unit weight of solid sorbent and the amount of solute remaining in the solution at equilibrium [36], [37]. Freundlich and Langmuir models were used to analyze the adsorption data obtained during the current study. The linear equation for Freundlich isotherm applied was [22]:

$$\text{Log } q_e = \log K_f + 1/n \log C_e \quad \ldots\ldots\ldots\ldots\ldots\ldots\ldots\ldots\ldots\ldots (3)$$

where K_f is correlated to the quantity of sorbate associated with the sorbent, and *n* is the Freundlich isotherm constant related to the strength of the sorption. A plot of log q_e vs. log C_e for SDS-bentonite and Na-bentonite is provided in Fig. 8 and the results are presented in Table 2. Generally, the Freundlich isotherm model is based upon the assumption that non-ideal adsorption occurs at heterogeneous surfaces; the latter arises from the presence of different functional groups on the surface as well as the various adsorbent-adsorbate interactions [35]. As well, this isotherm assumes that as the adsorbate concentration increases, the concentration of adsorbate onto adsorbent surface also increases and correspondingly, the sorption energy decreases upon the completion of the sorption centers of the adsorbent [12].

The two Freundlich constants (K_f and *n*) relate to the sorption capacity and adsorption energy distribution or sorption intensity of the sorbent (also known as the heterogeneity factor), respectively [35], [38]. The values obtained for K_f and *n* were reported to affect the adsorption isotherm, as the larger the values obtained indicate a higher adsorption capacity [39]. In addition, the magnitude of *n* gives was reported to give an indication of the favorability of adsorption where the favorable adsorption occurs when the *n* value was greater than unity [22]. Moreover, if *n* was less than unity, it implies that the adsorption process was chemical, but for *n* value above unity, the adsorption may be considered a favorable physical process [10].

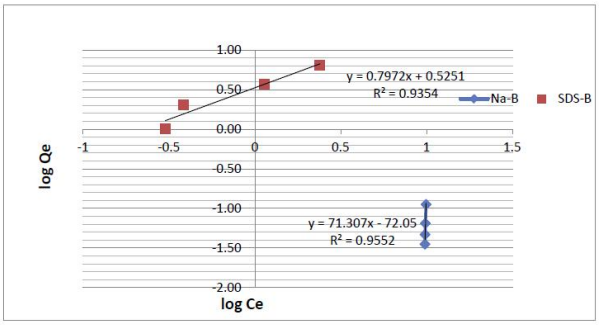

Fig. 8. Freundlich Isotherm for Na-B and SDS-B

International Journal of Scientific & Engineering Research Volume 6, Issue 3, March-2015
ISSN 2229-5518

TABLE 2
ISOTHERM CONSTANTS AND VALUES OF R^2 FOR SDS-B AND NA-B

Adsorbent	Freundlich isotherm			Langmuir isotherm			
	n (L/mg)	K_f (K mg/g)	R^2	Q_o (mg/g)	b (L/mg)	R_L	R^2
SDS-B	1.254	3.350	0.9354	16.556	2.67×10^{-1}	2.63×10^{-1}	0.6201
Na-B	1.403×10^{-2}	8.913×10^{-73}	0.9552	-8.99×10^{-4}	-9.987×10^{-2}	9.999×10^{-1}	0.8638

The Langmuir model, on the other hand, has been used to describe monolayer adsorption of the sorbate based on a kinetic approach and it assumes a uniform surface, single layer of adsorbed material occurring at a constant temperature [12]. As well, it assumes that all binding sites have the same affinity for adsorption of a single molecular layer and that there was no interaction between absorbent molecules [22]. The Langmuir isotherm utilized for the sorption equilibrium of SDS-bentonite and Na-bentonite was:

$$C_e/q_e = 1/b\,Q_0 + C_e/Q_0 \quad \text{..... (4)}$$

where Q_o and b are the Langmuir constants related to adsorption capacity and energy of adsorption, respectively. The Langmuir constant *b* reflects quantitatively the affinity between the adsorbent and adsorbate and the higher the value obtained, the higher the affinity for pollutant adsorption onto the adsorbent material [12]. The favorability of the adsorption process was reported to be dependent on the obtained value of separation factor (R_L) [10]. The dimensionless constant separation factor for equilibrium parameter, R_L, is an essential characteristic of the Langmuir isotherm which is defined as:

$$R_L = 1/(1 + bC_0) \quad \text{..... (5)}$$

where *b* is the Langmuir constant (L/mg) and C_o(mg/L) is the initial TOC concentration. There are 4 probabilities for the value of RL: for favorable adsorption $0<R_L<1$; for unfavorable adsorption $R_L>1$; for linear adsorption $R_L=1$ and for irreversible adsorption $R_L= 0$ [12]. A plot of C_e/q_e vs. C_e for both SDS-bentonite and Na-bentonite (Fig. 9) resulted in a straight line with a slope of $(1/Q_o)$ and an intercept of $1/bQ_o$. The values for the slope, intercept of this plot and R_L constant for each adsorbent are provided in Table 2. The results indicated the applicability of Langmuir model for adsorption of TOC onto SDS-bentonite due to the high value of correlation coefficient (R^2) as well as the R_L value indicated a favored adsorption. Furthermore, the Langmuir constant Q_o obtained showed that SDS-bentonite had a higher adsorption capacity or a higher estimated monolayer surface coverage towards TOC than Na-bentonite [22].

Overall, it is clear from the correlation coefficients (R^2) obtained for both SDS-B and Na-B that the experimental data fitted the Freundlich model. As well, it was reported that for Freundlich isotherm R^2 values greater than 0.9 this may be indicative of a multilayer adsorption with physisorption type process [40]. However, the value for n obtained for SDS-B reflect that the process was moderately difficult while that for Na-B, a value less than 1 reflects the fact the material had poor adsorbing characteristics [22].

Moreover, the Langmuir constant *b* can be used to calculate the thermodynamic parameters, which are associated with the adsorption process, on the basis of the following equation [10]:

$$\ln K_d = \Delta S^0/R \quad \Delta H^0/RT \quad \text{..... (6)}$$

where K_d is the single point or linear sorption distribution coefficient, ΔS^o is standard entropy (J/mol K), ΔH^o the standard enthalpy (kJ/mol), T is the absolute temperature (K), and R is the gas constant (8.314 J/mol K).

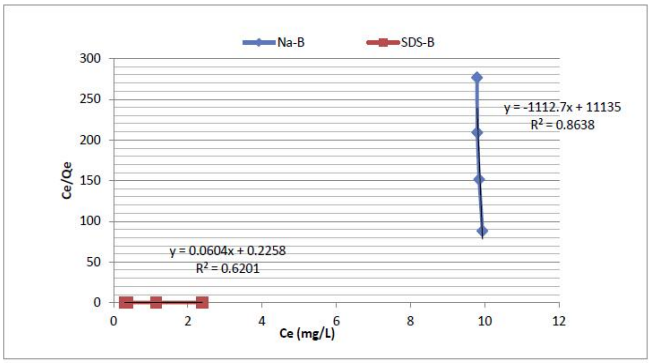

Fig. 9. Langmuir Isotherm for Na-B and SDS-B

The dimensionless equilibrium distribution coefficient K_d is defined as:

$$K_d = Q_e/C_e \quad \text{..... (7)}$$

where Q_e is the equilibrium adsorbate concentration on the adsorbent (mg L^{-1}) and C_e is the equilibrium adsorbate concentration in solution (mg L^{-1}). A plot of ln K_d versus 1/T rendered a straight line from which the values of ΔH^o and ΔS^o were calculated from the slope and intercept, respectively. The standard Gibbs free energy (ΔG^o, kJ/mol) was calculated using the following equation:

$$\Delta G^0 = \Delta H^0 - T\,\Delta S^0 \quad \text{..... (8)}$$

The results of the thermodynamic parameters are provided in Table 3.

TABLE 3
THERMODYNAMIC PARAMTERS FOR THE REMOVAL OF TOC USING NA-B AND SDS-B

Adsorbent	ΔH^o	ΔS^o	ΔG^o(kJ/mol)			
	(kJ/mol)	(kJ/mol. K)	298 °K	313 °K	323 °K	333 °K
SDS-B.	-20.98	-5.712×10^{-2}	-3.97	-3.10	-2.54	-1.97
Na-B.	-7.18	-7.083×10^{-2}	13.93	14.99	15.70	16.41

From the data in Table 3, the negative values of ΔH^o obtained for both SDS-B and Na-B indicates that the process is an exothermic process, which is in accordance with the findings of other researchers [10], [13], [16]. As well, the small negative value for ΔH^o for Na-B suggests that the adsorption is mainly a physical process involving weak forces of attraction [10], [41]. As well, it was reported that the value of the adsorption enthalpy may be used to distinguish between chemical and physical adsorption and that the latter ranged between 0 to 20 kJ/mol [41], such as was the case for Na-B.

The negative ΔS values obtained indicates that randomness

International Journal of Scientific & Engineering Research Volume 6, Issue 3, March-2015
ISSN 2229-5518

decreased at the solid–solution interface during the adsorption of TOC onto both materials, i.e. the molecules in solution had more freedom relative to those attached to the surface [41]. As well, the small decrease in entropy may indicate that the change in enthalpy was not large enough to compensate for this change in randomness. Overall, obtaining negative ΔH and ΔS values suggests that enthalpy contributes more than entropy in producing negative ΔG values [42]. On the other hand, with ΔH and ΔS having negative values, this may indicate that the process was considered spontaneous for $T < \Delta H/\Delta S$, in this case less than 100 K.

From the data in Table 3, ΔG^o obtained for SDS-B ranged had negative values which indicate the feasibility and spontaneity of TOC adsorption onto this material [10], [43]. As well, it was observed that this ΔG^o negative value decreased with the increase in temperature which may indicate that the adsorption process on SDS-B was more favorable at higher temperatures [44]. Furthermore, the negative ΔG values imply that the reaction should proceed in the direction of product formation [45]. On the other hand, the positive value for ΔG^o for Na-B adsorption of TOC indicates that the process was not spontaneous. In addition, the increase in the free energy values for Na-B going from 25- 60 °C may indicate that the adsorption process was energetically less favorable at higher temperatures [41].

It was reported that a change in free energy (ΔG^o) between -20 and 0 kJ mol^{-1} was indicative of a physisorption process [10], [41], whereas for a chemisorption process, the values ranged between -80 to 400 kJ mol^{-1} [10]. Concerning the values of (ΔG^o) obtained for SDS-B, they were within the middle of physisorption and chemisorption range which may indicate that the process may be interpreted as a physical adsorption enhanced by a chemical effect [10]. However, the value for (ΔG^o) obtained for Na-B may indicate that it is a physisorption process. Furthermore, the increase in the positive value of ΔG^o for Na-B with the increase in temperature may indicate that the adsorption process becomes energetically less favorable at higher temperatures [41]. It was indicated that irreversible adsorption occurs with chemical groups' interaction whereas with a physical process, it was a reversible [46].

The activation energy for TOC adsorption onto SDS-bentonite and Na-bentonite was calculated using the Arrhenius equation:

$$\ln k = \ln A_0 \quad E_a/RT \qquad (9)$$

where A_o is the Arrhenius constant, regardless of temperature, E_a the activation energy (kJ/mol) and R is the gas constant (8.314 J/mol K). A plot of ln k vs 1/T for each adsorbent, indicated the activation energy for TOC adsorption onto SDS-bentonite was -22.41 kJ/mole, while that for Na-bentonite, it was -49.06kJ/mole. The negative value of activation energy indicates that the reaction was exothermic and that the rise in the solution temperature did not favor the sorption process [47], [48]. As well, negative activation energy indicates the absence of an energy barrier for the adsorption to occur and that with the increase in temperature, there was a reduction in colliding molecules to capture one another [48].

3.7 Adsorption Kinetics:

Four kinetic models, namely: pseudo-first order, pseudo-second order, Weber and Morris intraparticle diffusion model and Bangham's pore diffusion model were applied to identify the rate and kinetics of TOC sorption onto SDS-B and Na-B. The process was studied at (25, 40, 50 and 60 ºC) using variable contact time, pH = 5 and an initial TOC_o concentration of 10.5 mg/L. The linear first-order Lagergren rate equation expression used was [22]:

$$\log(q_e - q_t) = \log(q_e) - k_1 t/2.303 \qquad (10)$$

where q_e and q_t (mg/g) are the adsorption capacities at equilibrium and at time t, respectively. The rate constant k_1 (min^{-1}) and the process activation energy were obtained from the slope of the plot of log (qe–qt) vs. t for each adsorbent. This model assumes that the rate of change of adsorbate uptake with time is directly proportional to the difference in the saturation concentration and the amount of solid uptake with time. The pseudo second order model, on the other hand, is based upon the sorption capacity on the solid phase [35]. The second-order rate equation applied was:

$$t/q_t = 1/k_2 q_e^2 + t/q_e \qquad (11)$$

where k_2 is the rate constant of second-order adsorption and the slopes of the plots of t/qt versus t were used to determine the second order rate constant k_2 as well as the process activation energy. The values for the kinetic parameters calculated for the pseudo-first and pseudo-second rate of reaction for the adsorption process are provided in Table 4.

The data in Table 4 revealed that the sorption of TOC onto both SDS-bentonite and Na-bentonite was best fitted to pseudo-second order kinetics rather than the first order model. The data also indicated that the calculated (q_e) values for the 2nd order rate were in accordance with those obtained from the experimental runs as well as the correlation coefficients (R^2) were close to unity. However, the difference between the experimental and calculated values for q_e for the pseudo-first order model relative to the second order model may be attributed to a possible time lag caused by a boundary layer or external resistance that controls the sorption process at the beginning [35]. The plots for pseudo-second order rate for both SDB-B and Na-B (not shown here) indicated a best fit over the whole data range which may indicate that the rate limiting step was a chemical adsorption process between TOC and the ogranophilic bentonite and bentonite [27], [35]. As well, it was observed that for Na-B there was a significant decrease in the value of K_2 going from 25 °C to 65°C which may be indicative of an exothermic process [10], [16]. In addition, it may be indicative of the fact that the increase in temperature weakened the adsorptive forces between the active sites of the absorbent and the adsorbate as well as between the adjacent molecules of the adsorbed species [10], [16].

It was reported that the transport of adsorbate from the liquid phase to the solid phase may occur via different mecha-

International Journal of Scientific & Engineering Research Volume 6, Issue 3, March-2015
ISSN 2229-5518

nisms that may be controlled by either pore or film diffusion and mass action [16], [27], [49]. In many adsorption processes, the adsorbate species may most probably be transported from the bulk of the solution into the solid phase through intra-particle diffusion/transport [27], [49]. Accordingly, the intra-particle (Weber and Morris) diffusion model was examined as per the following equation [12]:

$$q_t = k_i t^{0.5} + I \quad \text{..... (12)}$$

where q_t is the fraction of pollutant uptake (mg/g) at time *t*, k_i is the intra-particle-diffusion rate constant (mg/g $min^{0.5}$) and *I* is the intercept (mg/g). A plot of q_t vs. $t^{0.5}$ provided the values for k_i and intercept *I* that are listed in Table 4. In general, the value of the intercept provides some information about the thickness of the boundary layer and the larger the intercept the greater the boundary effect [35]. Overall, for all plots drawn, no zero intercept was obtained which may be indicative of some degree of boundary layer control and that may be operating simultaneously with other kinetic models to control the rate of adsorption [12], [27]. As well, it was observed that the correlation coefficients (R^2) obtained for the intraparticle diffusion model for both materials were more 0.810, which reflects that surface adsorption and intraparticle diffusion were concurrently operating during the adsorption process [12]. However, the effect of intraparticle diffusion upon TOC sorption onto Na-B was more as the temperature increased which indicates the fact that kinetically energetic molecules were able to be adsorbed onto it.

On the other hand, it was observed that the plot for q_t vs. $t^{0.5}$ for Na-B was curved initially which was followed by a linear portion. This noted curvature in the shape of the plot at a small time limit was reported to be due to mass transfer resistance and bulk diffusion while the linear portion may be attributed to intra-particle /pore diffusion [12], [27]. In order to assess the effect of pore diffusion during the process of TOC sorption onto SDS-B and Na-B, the Bangham's equation applied was [50]:

$$\log\log[C_i/(C_i - q_t m)] = \log[k_0 m/2.303V] \quad \text{.....(13)}$$

where C_s the weight of adsorbent used per liter of solution (mg/L), V (mL) is volume of solution, m (g/L) is the weight of adsorbent per liter of solution, q_t (mg/g) is the amount of adsorbate retained at time t and α (<1) and k_o are constants. Log [C_i/C_i –M qt] was plotted against log t and the plots obtained were not linear for both SDS-B and Na-B. This may indicate that the adsorption kinetics was not limited only by pore diffusion [50]. The values of k_o and σ along with the correlation coefficient are presented in Table 4. According to the obtained correlation coefficients (R^2) for TOC adsorption onto Na-B, it is clear that both film and pore diffusion did contribute significantly to the different stages of the sorption mechanism.

TABLE 4
KINETIC PARAMTERS CALCULATED FOR THE REDUCTION OF TOC USING NA-B AND SDS-B AT DIFFERENT TERMPERATURES (°K), WHERE R^2 IS THE CORRELATION COEFFICIENT

Adsorbent	Temp (°K)	Pseudo-first-order			Pseudo-second-order			Intra-particle Diffusion			Bangham model		
		K_1 (min^{-1}) x10^{-2}	q_e (mg/g) 10^{-2}	R^2	K_2 (g mg^{-1} min^{-1}) x 10^{-1}	q_e (mg/g)	R^2	K_i(mg g^{-1} $min^{-0.5}$) x10^{-3}	I (mg/g)	R^2	k_o (mL L^{-1} g^{-1})	α	R^2
SDS-B	298	3.616	8.097	0.8551	18.609	2.029	0.9997	17.40	1.9154	0.8488	473.07	0.0795	0.6864
	313	3.616	14.976	0.8558	9.727	1.970	0.9990	32.30	1.7587	0.8495	352.80	0.1007	0.6928
	323	3.316	14.827	0.8539	9.590	1.969	0.9989	32.00	1.7577	0.8325	352.55	0.0996	0.6728
	333	2.856	13.925	0.9135	9.946	1.962	0.9989	30.30	1.7599	0.8175	354.92	0.0936	0.6568
Na-B	298	11.40	2.580	0.9702	98.56	3.71 x10^{-2}	0.9997	2.50	1.86	0.8720	1.67	0.2412	0.8674
	313	7.001	2.240	0.9750	42.55	3.53x 10^{-2}	0.9995	3.40	7.80	0.8749	7.31 x 10^{-1}	0.4727	0.8395
	323	9.995	3.853	0.9469	22.79	3.44x 10^{-2}	0.9973	3.70	2.20	0.9380	3.82 x 10^{-1}	0.6384	0.8851
	333	6.149	3.149	0.9317	12.22	3.67x 10^{-2}	0.9815	3.80	-1.10	0.9896	2.52 x 10^{-1}	0.7385	0.9380

4 CONCLUSION

In the current work, the adsorption of TOC from liquid solutions onto Na-bentonite and SDS-bentonite was investigated. The results showed that the experimental data was well represented by the second order kinetic model for both SDS-bentonite and Na-bentonite. As well, the data revealed that the process did involve some intraparticle diffusion for SBS-B. However, for NA-B, the results indicated that both intraparticle and pore diffusion significantly contributed or were the rate controlling steps f the overall adsorption process specifically at higher temperatures. The equilibrium data for both SDS-bentonite and Na-B were better fitted to Freundlich model. The apparent activation energies calculated for this process were -49.06 kJ/mol and -22.41 kJ/mol for Na-bentonite and SDS-bentonite, respectively. Thermodynamicaly the process was exothermic and spontaneous in the forward direction (irreversible) for SDS-bentonite while its was spontaneous in the backward direction (reversible) for Na-bentonite. The results also indicated a higher TOC removal using modified SDS-bentonite was more favored over Na-B due to its organophilic behavior after modification and smaller particle size.

REFERENCES

[1] A. H. Sulaymon, A-F. M. Ali and S. K. Al-Naseri, "Natural organic matter removal from Tigris River water in Baghdad, Iraq", Desalination 245, pp. 155–168, 2009.

[2] A. Matilainen, M. Vepsäläinen and M. Sillanpää, "Natural organic matter removal by coagulation during drinking water treatment: A review", Advances in Colloid and Interface Science 159, pp. 189–197, 2010.

[3] R. Fabris, C. W. K. Chow, M. Drikas and B. Eikebrokk, "Comparison of NOM character in selected Australian and Norwegian drinking waters", Water Research 42, pp. 4188-4196, 2008.

[4] L. Joseph, J. R.V. Flora, Y-G. Park, M. Badawy, H. Saleh and Y. Yoon, "Removal of natural organic matter from potential drinking water sources by combined coagulation and adsorption using carbon nanomaterials", Separation and Purification Technology 95, pp. 64–72, 2012.

[5] A. Matilainen and M. Sillanpää, "Removal of natural organic matter from drinking water by advanced oxidation processes", Chemo-

International Journal of Scientific & Engineering Research Volume 6, Issue 3, March-2015
ISSN 2229-5518

sphere 80, pp. 351–365, 2010.

[6] A. Matilainen, E. T. Gjessing, T. Lahtinen, L. Hed, A. Bhatnagar and M. Sillanpää, "An overview of the methods used in the characterisation of natural organic matter (NOM) in relation to drinking water treatment", Chemosphere 83, pp. 1431–1442, 2011.

[7] C. Wang, X. Jiang, L. Zhou, G. Xia, Z. Chen, M. Duan and X. Jiang, "The preparation of organo-bentonite by a new gemini and its monomer surfactants and the application in MO removal: A comparative study", Chemical Engineering Journal 219, pp. 469–477, 2013.

[8] F. Xiao, X. Zhang, H. Zhai, M. Yang and I. M.C. Lo, "Effects of enhanced coagulation on polar halogenated disinfection byproducts in drinking water", Separation and Purification Technology 76, pp 26–32, 2010.

[9] I. Kristiana, C. Joll and A. Heitz, "Powdered activated carbon coupled with enhanced coagulation for natural organic matter removal and disinfection by-product control: Application in a Western Australian water treatment plant", Chemosphere 83, pp. 661–667, 2011.

[10] A. Özcan, Ç. Ömeroğlu, Y. Erdoğan and A. S. Özcan, "Modification of bentonite with a cationic surfactant: An adsorption study of textile dye Reactive Blue 19", J of Haz. Mat. 140, pp. 173–179, 2007.

[11] X. Sun, W. Huang, Z. Ma, Y. Lu and X. Shen, "A novel approach for removing 2-naphthol from wastewater using immobilized organobentonite," J of Haz. Mat. 252– 253, pp 192– 197, 2013.

[12] F. M. S. E. El-Dars; M. H. M. Bakr and A. M. E. Gabre, "Reduction of COD in Resin Production Wastewater Using Three Types of Activated carbon". Journal of Environmental Treatment Techniques Volume 1, Issue 3, pp. 126-136, 2013.

[13] S. Al-Asheh; F. Banat; L. Abu-Aitah (2003). Adsorption of phenol using different types of activated bentonites. Separation and Purification Technology 33, 1-10.

[14] Asem A. Atia, F. M. Farag and A. E-F. M.Youssef, "Studies on the adsorption of dodecylbenzenesulfonate and cetylpyridinium bromide at liquid/air and bentonite/liquid interfaces", Colloids and Surfaces A: Physicochem. Eng. Aspects 278, pp. 74–80, 2006.

[15] J. Ma, J. Qi, C. Yao, B. Cui, T. Zhang and D. Li, "A novel bentonite-based adsorbent for anionic pollutant removal from water", Chemical Engineering Journal 200–202, pp. 97–103, 2012.

[16] T.S. Anirudhan and M. Ramachandran, "Surfactant-modified bentonite as adsorbent for the removal of humic acid from wastewaters", Applied Clay Science 35, pp. 276–281, 2007.

[17] J. Ma and L. Zhu, "Removal of phenols from water accompanied with synthesis of organobentonite in one-step process", Chemosphere 68, pp. 1883–1888, 2007.

[18] S. Tunç, O. Duman and B. Kanci, "Rheological measurements of Na-bentonite and sepiolite particles in the presence of tetradecyltrimethylammonium bromide, sodium tetradecyl sulfonate and Brij 30 surfactants", Colloids and Surfaces A: Physicochem. Eng. Aspects 398, pp. 37– 47, 2012.

[19] Y. Zhang, Y. Zhao, Y. Zhu, H. Wu, H. Wang and W. Lu, "Adsorption of mixed cationic-nonionic surfactant and its effect on bentonite structure", Journal of Environmental Sciences 24(8), pp. 1525–1532, 2012.

[20] T. Elford and D. J. Pernitsky, *Case Study 4: NOM Measurements for Coagulation Control*, in *Operational Control of Coagulation and Filtration Processes,* 3rd Ed., AWWA, pp 163-165, 2011.

[21] American Public Health Association (APHA), "*Standard Methods For the Examination of Water and Wastewater*, American Public Health Association, 22nd ed., Washington D.C., USA, 2012.

[22] F. M. S. E. El-Dars; A-E. O. Sayed; B.A. Salah and M. E. H. Shalabi, "Removal of Nickel (II) from aqueous solution via carbonized date pits and carbonized rice husks", Eurasian Chem Tech Journal 13, pp. 267-277, 2011.

[23] S. Yang, J. Li, Y. Lu, Y. Chen and X. Wang, "Sorption of Ni(II) on GMZ bentonite: Effects of pH, ionic strength, foreign ions, humic acid and temperature", Applied Radiation and Isotopes 67, pp. 1600–1608, 2009.

[24] R. B. Viana, A. B. F. da Silva and A. S. Pimentel, "Infrared Spectroscopy of Anionic, Cationic, and Zwitterionic Surfactants", Advances in Physical Chemistry Volume 2012, Article ID 903272, 14 pages doi:10.1155/2012/903272.

[25] G. Akçay and M. Kadir Yurdakoç, "Nonyl-and Dodecylamines Intercalated Bentonite and Illite from Turkey", Turk J Chem 23, pp.105 – 113, 1999.

[26] T. Yalçın, A. Alemdar, Ö .I. Ece and N. Güngör, "The viscosity and zeta potential of bentonite dispersions in presence of anionic surfactants" Materials Letters 57, pp. 420–424, 2002.

[27] A. Khenifi, Z. Bouberka, K. Bentableb, H. Hamani and Z. Derriche, "Removal of 2,4-DCP from wastewater by CTAB/bentonite using one-step and two-step methods: A comparative study", Chemical Engineering Journal 146, pp. 345–354, 2009.

[28] N. S. Gunawan, N. Indraswati, Y-H. Ju, F. E. Soetaredjo, A. Ayucitra and S. Ismadji, "Bentonites modified with anionic and cationic surfactants for bleaching of crude palm oil", Applied Clay Science 47, pp. 462–464, 2010.

[29] H. Omar, H. Arida and A. Daifullah, "Adsorption of ^{60}Co radionuclides from aqueous solution by raw and modified bentonite", Applied Clay Science 44, pp. 21–26, 2009.

[30] M A. Akl, AM Youssef and MM Al-Awadhi, "Adsorption of Acid Dyes onto Bentonite and Surfactant-modified Bentonite", J Anal Bioanal Tech 4: 174. doi:10.4172/2155-9872.1000174, 2013.

[31] E Günister, S Işçi, A Alemdar and N Güngör, "Effect of sodium dodecyl sulfate on flow and electrokinetic properties of Na-activated bentonite dispersions", Bull. Mater. Sci., Vol. 27, No. 3, pp. 317–322, 2004.

[32] S. E-S. Ghazy, A. A. El-Asmy and A. M. EL-Nokrashy, "Batch Removal of Nickel by Eggshell as a Low Cost Sorbent", Int. J. Ind. Chem., Vol. 2, No. 4, pp. 242-252, 2011.

[33] S.S. Tahir and R. Naseem, "Removal of Cr(III) from tannery wastewater by adsorption onto bentonite clay", Separation and Purification Technology 53, pp. 312–321, 2007.

[34] A. Syafalni, A. Yusof, R. Abdullah and I. Abustan, "Enhancement Of Dye Waste Treatment Using Fenton's Reagent And Adsorbents (Natural Bentonite, Surfactant Modified Bentonite And Activated Carbon)", International Journal Of Environmental Sciences Volume 4, No 5, pp. 801-815, 2014.

[35] M Sathishkumar, A R Binupriya, D Kavitha, R Selvakumar, K K Sheema, J G Choi and S E Yun, "Organic micro-pollutant removal in liquid-phase using carbonized silk cotton hull", Journal of Environmental Sciences 20, pp. 1046–1054, 2008.

[36] S. M. Dal Bosco; R. S. Jimenez and W. A. Carvalho, "Removal of toxic metals from wastewater by Brazilian natural scolecite", Journal of Colloid and Interface Science 281, pp. 424-431, 2005.

[37] D. Sud; G. Mahajan and M. P. Kaur, "Agricultural Waste Material as potential adsorbent For Sequestering Heavy Metal Ions from Aqueous Solutions-A Review", Bioresource Technology 99, pp. 6017-6027, 2008.

International Journal of Scientific & Engineering Research Volume 6, Issue 3, March-2015
ISSN 2229-5518

[38] S. Chowdhury, R. Mishra, P. Saha and P. Kushwaha, "Adsorption thermodynamics, kinetics and isosteric heat of adsorption of malachite green onto chemically modified rice husk", Desalination 265, pp. 159–168, 2011.

[39] M. Bansal; D. Singh; V.K Garg and P. Rose, " Use of agricultural waste for the removal of Nickel Ions from Aqueous Solutions: Equilibrium and Kinetics Studies", International Journal of Civil and Environmental Engineering 1: 2, pp. 108-114, 2009.

[40] P. K Pandey; S. Choubey; Y. Verma; M. Pandey; S. S. K Kamal and K. Chandrashekhar, "Biosorptive Removal of Ni(II) from Wastewater and Industrial Effluent", Int. J. Environ. Res. Public Health 4(4), pp. 332-339, 2007.

[41] H. Al-Omari, "Evaluation of the Thermodynamic Parameters for the Adsorption of Cadmium Ion from Aqueous Solutions", Acta Chim. Slov. 54, pp. 611–616, 2007.

[42] J. S. Piccin, G. L. Dotto and L. A. A. Pinto "Adsorption Isotherms And Thermochemical Data Of Fd&C Red N° 40 Binding By Chitosan", *Brazilian Journal Of Chemical Engineering*, Vol. 28, No. 02, pp. 295 – 304, 2011.

[43] J.M. Salman, V.O. Njoku and B.H. Hameeda, "Batch and fixed-bed adsorption of 2,4-dichlorophenoxyacetic acid onto oil palm frond activated carbon", Chemical Engineering Journal 174, pp. 33– 40, 2011.

[44] J. He, S. Hong, L. Zhang, F. Gan and Y- Ho, "Equilibrium and Thermodynamic Parameters of Adsorption of Methylene Blue Onto Rectorite", Fresenius Environmental Bulletin Volume 19, No 11a, pp. 2651- 2656, 2010.

[45] E. R. Mouta, M. R. Soares and J. C. Casagrande, "Copper Adsorption as a Function of Solution Parameters of Variable Charge Soils", J. Braz. Chem. Soc., Vol. 19, No. 5, pp. 996-1009, 2008.

[46] M. Domingo-García, A.J. Groszek, F.J. López-Garzón and M. Pérez-Mendoza, "Dynamic adsorption of ammonia on activated carbons measured by flow microcalorimetry", Applied Catalysis A: General 233, pp. 141–150, 2002.

[47] M. Al-Ghouti; M. A. M. Khraisheh; M. N. M. Ahmad and S. Allen, "Thermodynamic behaviour and the effect of temperature on the removal of dyes from aqueous solution using modified diatomite: A kinetic study",Journal of Colloid and Interface Science 287, pp. 6–13, 2005.

[48] R. Kobiraj, N. Gupta, A. K. Kushwaha and M C Chattopadhyaya, "Determination of equilibrium, kinetic and thermodynamic parameters for the adsorption of Brilliant Green dye from aqueous solution onto egg shell powder", Indian Journal of Chemical Technology, 19, pp. 26-31, 2012.

[49] H. Qiu, Lu Lv, B-C. Pan, Q-J. Zhang, W-M. Zhang and Q-X. Zhang, "Critical Review in Adsorption Kinetic Models", J Zhejiang Univ Sci A 10(5), pp. 716-724, 2009.

[50] Z.L. Yaneva, B.K. Koumanova and S.J. Allen, "Applicability comparison of different kinetic/diffusion models for 4-nitrophenol sorption on Rhizopus oryzae dead biomass", Bulgarian Chemical Communications, Volume 45, Number 2, pp. 161 – 168, 2013.